

Structure and texture of alumina aerogel monoliths made by complexation with ethyl acetoacetate

A. PIERRE

Institut de Recherches sur la Catalyse, CNRS-UPR 5401, Université Claude Bernard—Lyon I, 2 avenue Albert Einstein 69626, Villeurbanne Cedex, France

R. BEGAG*, G. PAJONK

LACE, CNRS-UMR 5634—Université Claude Bernard—Lyon I, 69622, Villeurbanne Cedex, France

E-mail: apierre@catalyse.univ-lyon1.fr

Alumina gels can be made by spontaneous gelation of alkoxides in organic solvents, their hydrolysis rate can be controlled by chelating agents and the wet gels obtained can be transformed to aerogels by supercritical drying. The present study reports on such alumina aerogels made from aluminum tri-sec-butoxide in organic solvent and complexed with ethylacetoacetate at high temperature ($\approx 260^\circ\text{C}$) in methanol. The aerogels were studied by X-ray diffraction, nitrogen adsorption, infra-red spectroscopy and ^{27}Al nuclear magnetic resonance. The results show that both the chemical complexation and drying methods can significantly affect the texture and structure of these gels. © 1999 Kluwer Academic Publishers

1. Introduction

The synthesis of silica gel monoliths, either as xerogels or as aerogels has been extensively reported. On the contrary, publications on the synthesis of alumina gel monoliths are more limited. The most outstanding success was as small xerogel monoliths by Yoldas [1]. The difficulty in making such samples is related to the fact that alumina gels are usually made in excess water and they consist of a phase which is related to boehmite $\gamma\text{-AlO}(\text{OH})$ and soluble in water. Consequently, gelation can only be achieved if water is eliminated either by evaporation or by dialysis in an organic solvent.

In the present report a synthesis technique different from the Yoldas one was used, as spontaneous gelation of aluminum secondary butoxide was studied in acetone with the help of an organic complexing additive. Such gels could then directly be dried by the supercritical method in methanol at high temperature ($\approx 260^\circ\text{C}$) to obtain aerogels, instead of xerogels. The materials which were obtained are described from the point of view of their structure and pore texture in the dry state. In particular, in order to try understanding the role of etac in the formation of the gel network, samples with different $[\text{etac}]/[\text{Al}]$ and $[\text{solvent}]/[\text{Al}]$ ratio were made, and they were studied by X-ray diffraction (XRD) Fourier transform infra-red absorption (FTIR), and nuclear magnetic resonance (NMR).

2. Experimental

Alumina gels were synthesized by sol-gel according to conditions which are summarized in Table I. In this table, as well as in all further tables, the data for samples AAa60/260 and AAa50/35 made in a previous study [2] were added. In all samples, the Al precursor was aluminum sec-butoxide (Al-sb), the solvent was acetone and ethyl acetoacetate (etac) was added in this solvent as a complexing agent, before mixing with the alkoxide. This organic additive made it possible to slow down the hydrolysis of Al-sb in a further step. Three different molar ratio $[\text{acetone}]/[\text{Al-sb}]$ were studied; each corresponded to series respectively labeled a, b and c, as indicated in Table I. For each Al-sb dilution, three different molar proportions $[\text{etac}]/[\text{Al-sb}]$ were examined: ≈ 1 ; ≈ 1.5 and ≈ 2.1 . Hydrolysis was always carried out with the same water molar ratio $[\text{H}_2\text{O}]/[\text{Al-sb}] \approx 2.6$ in all samples and a small quantity of ammonia was always added as a catalyst, because a previous study showed that this catalyst somewhat enhanced obtaining monoliths [2].

For all samples except AAa50/35, gelation was achieved by bringing the solution at $T \approx 60^\circ\text{C}$ in a thermal bath and it always occurred in less than 24 h. All gels were dried by the supercritical method in methanol at $T \approx 260^\circ\text{C}$ according a method initially designed by Teichner *et al.* [3, 4]. For this purpose, test tubes containing the gels to dry were placed in an autoclave. A known volume of methanol, in excess by

* Present address: Aspen Systems, Marlborough, Mass, 01752, USA.

TABLE I Synthesis conditions of wet gels

Sample	Al-sb mass (g)	Molar ratio acetone/Al	Molar ratio Etac/Al	Molar ratio H ₂ O/Al	Molar ratio NH ₃ /Al
w	20.6	6.5	1.2	2.6	1.6×10^{-2}
x	10	6.7	1.2	2.6	3.2×10^{-2}
AAa60/260	10	6.7	1.2	1.2	3.2×10^{-2}
AAa50/35	10	6.7	1.2	1.2	3.2×10^{-2}
a1	7.51	6.7	1	2.6	8.5×10^{-2}
a2	7.68	6.5	1.5	2.5	8.3×10^{-2}
a3	7.50	6.7	2.1	2.6	8.5×10^{-2}
b1	9.39	5.3	1	2.6	6.8×10^{-2}
b2	9.43	5.3	1.6	2.6	6.8×10^{-2}
b3	9.38	5.4	2.1	2.6	6.8×10^{-2}
c1	11.46	4.4	1	2.6	5.6×10^{-2}
c2	11.21	4.5	1.5	2.6	5.7×10^{-2}
c3	11.24	4.5	2.1	2.6	5.7×10^{-2}

comparison with the volume of gel samples (400 cm^3 versus $\approx 20 \text{ cm}^3$ gel volume), was added. After closure, the autoclave was purged with nitrogen. Then it was heated until its temperature reached $\approx 260^\circ\text{C}$, while its pressure spontaneously increased to $\approx 120 \text{ atm.}$, well above the critical point of pure methanol (242°C and 79 atm.). These conditions were maintained for several hours before evacuating the autoclave. Although the initial gel solvent, acetone, increases the critical point pressure and temperature of methanol, it also exchanges well with this alcohol, so that the wet gels ended up containing the same supercritical methanol solution as the entire autoclave. This supercritical fluid could be evacuated as a gas, an operation which was carried out very slowly to maintain the temperature at a level making possible to avoid cutting the coexistence line between liquid and vapor methanol, inside the autoclave. The evacuated supercritical fluid was cooled and condensed after leaving the autoclave and the volume of liquid which was recovered gave another indication of the proper drying of gels. The autoclave was opened after flushing with nitrogen and after its temperature had decreased to a reasonable value. No liquid remained inside and the brittle samples which remained did not lose any further mass when let in open air, which provided another indication that they were dry. The only processing difference between sample AAa50/35 and all other samples, is that gelation was achieved at 50°C and supercritical drying was done in liquid CO_2 at much lower temperature ($\approx 35^\circ\text{C}$).

The nature of phases in all aerogels was analyzed by powder X-ray diffraction in a Siemens D500 diffractometer using the $\text{CuK}\alpha$ radiation. Such analyses were carried out just after drying a gel, then after a heat treatment in air at 900°C for 5 h (heating and cooling rates $\approx 5^\circ\text{C}/\text{min}$ in an air flow $\approx 6 \text{ L/h}$). The main characteristics of the samples, concerning their monolithic aspect and transparency, were recorded. The specific surface of a very small solid piece of each sample, before and after heat treatment at 900°C , was determined by the Bruauer Emmett and Teller (BET) method on a customized piece of equipment. All samples were previously desorbed at 300°C for 5 h before measuring the

specific surface are (except 4 h at 400°C for samples AAa60/260 and AAa50/35). Infra-red absorption data were obtained on a Fourier transform FTIR Vector 22 from Bruker, under nitrogen, and NMR data on a DSX 400 MHz from Bruker.

3. Results

The characteristics of all aerogels are summarized in Table II. The typical aspect of a wet gel before supercritical drying, labeled gel w in Table I, is illustrated in Fig. 1a. If such a wet gel is very slowly dried by evaporation in air, a transparent xerogel monolith with a bright orange color is obtained, such as the xerogel labeled x in Table I and shown in Fig. 1a. Xerogel x was slowly dried in about two years through a porous tube closure to reach the state illustrated in Fig. 1a. All wet gels, apart from AAa50/35, shrunk by $\approx 25\%$ during transformation to aerogels by supercritical drying, as this is illustrated in Fig. 1b for the series b samples, shown in their original test tube. This figure shows that they were small, brown, opaque or partly translucent rods. The biggest single monoliths were obtained in the series b and with sample c1. However, extensive microcracking was obvious in these monoliths, which had to be handled with great care. These rods shrunk more ($\approx 25\%$ from visual observations) after thermal treatment at 900°C , but they lost their coloration (Fig. 1c). Simultaneously, their handling strength and their translucency improved significantly during such heat treatments. The

TABLE II Characteristics of aerogels and heat treated samples

Sample	Characteristic of wet gel	Characteristic of aerogel monolith	Characteristic at 900°C
w	Clear, slightly yellow		
x	Clear, slightly yellow	Orange, transparent xerogel monolith	
AAa60/260	Clear, slightly yellow	Brown, translucent fractured	Partly transparent fractured
AAa50/35	Clear, slightly yellow	Very light slightly yellow fluffy small aggregates (a few mm in size)	Translucent fluffy aggregates
a1	Opaque, slightly yellow	Brown, opaque, fractured	Partly transparent fractured
a2	Clear, slightly yellow	Brown, opaque, fractured	White translucent fractured
a3	Clear, slightly yellow	Brown, opaque, fractured	White translucent fractured
b1	Opaque, slightly yellow	Dark brown, slightly translucent, fractured	Transparent
b2	Clear, slightly yellow	Brown, slightly translucent, fractured	Partly transparent fractured
b3	Clear, slightly yellow	Brown, slightly translucent, fractured	White translucent fractured
c1	Opaque, slightly yellow	Brown, slightly translucent, fractured	White translucent fractured
c2	Clear, slightly yellow	Brown, slightly translucent, fractured	Transparent
c3	Clear, slightly yellow	Brown, slightly translucent, fractured	White translucent fractured

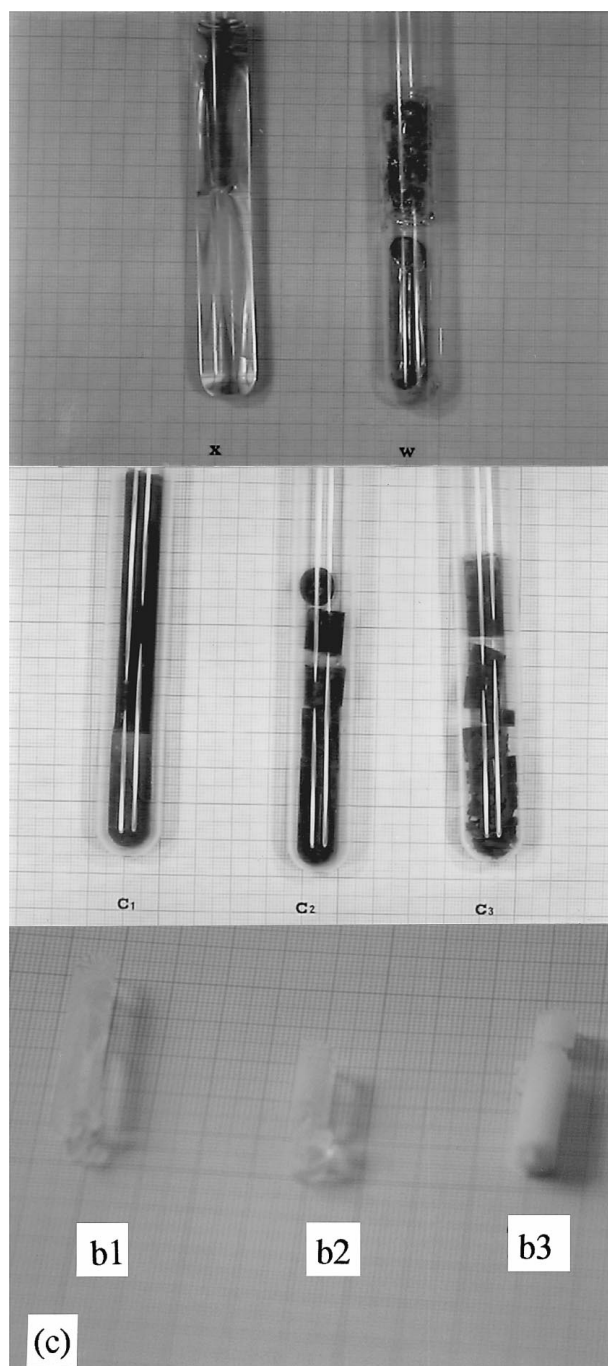


Figure 1 Photographs of gels made by the synthesis technique used in the present study: (a) wet alumina gel (w) and a xerogel (x); (b) gels after supercritical drying in methanol; (c) of aerogels heat treated at 900 °C in air.

main characteristics of these aerogels are summarized in Table II. All samples turned white and opaque at 1200 °C. Sample AAa50/35 dried in supercritical CO₂ did not really shrink, but it broke in tiny fluffy aggregates.

The X-ray diffraction patterns characteristics of aerogels just after drying and after heat treatment at 900 °C, are summarized in Fig. 2. Just after drying, three types of different XRD patterns were observed:

- A pseudo-boehmite type for samples a1, a2 and c1, where the main boehmite interlayer (020) peak was displaced at a smaller angle, as this can be seen by comparison with a Yoldas type Y sample.

- A very weak pseudo-boehmite type XRD pattern as in samples b1, c2 and c3, where the boehmite interlayer (020) peak was only a weak shoulder on the central diffraction peak, at roughly the same small angle value as for previous samples, and all other peaks actually were slight bumps on the XRD pattern.
- An amorphous one for sample a3, b2 and b3, AAa60/260 and AAa50/35.

In all samples where a pseudo-boehmite XRD pattern was observed, the interlamellar (020) peak, or the shoulder on the central peak for the weak pseudo-boehmite samples, had shifted from $2\theta \approx 14^\circ$ according to the JCPDS file in agreement with the Y sample pattern, down to a smaller angle $2\theta \approx 11^\circ$. On the other hand, all other boehmite peaks were broad but they remained at the same 2θ angle as in the JCPDS data file. The amorphous samples had an X-ray pattern with a single and very broad maximum, at a 2θ angle $\approx 24.5^\circ$, difficult to attribute to any known file of aluminum hydroxide related phase. At 900 °C, the same transition phase related to δ -alumina had formed in all samples.

The BET specific surface areas of the aerogels just after drying and after heat treatment are gathered in Figs 3 and 4 respectively. As shown in Fig. 3, the specific area just after supercritical drying at $\approx 260^\circ\text{C}$, followed by outgasing at 300 °C, tended to increase as the [solvent]/[Al] ratio decreased and the molar ratio [Etac]/[Al] increased. On the other hand, the residual specific surface area after heat treatment at 900 °C appears to be roughly independent of the initial one (Fig. 4).

In Fig. 5, the pore size distributions of samples AAa60/260 and AAa50/35 made in a preceding study [2] are joined. The first of these two samples was done by exactly the same technique as all other samples in the present study, while the second sample only differed by supercritical drying in liquid CO₂, a liquid which is known to exchange well with acetone. The purpose of this figure is to show that the dominating pore size shifted to a larger value, from ≈ 10 to ≈ 14 nm, when the supercritical drying temperature was lowered from 260 °C in methanol, to $\approx 35^\circ\text{C}$ in CO₂.

FTIR transmission spectra for the dry gels are reported in Fig. 6, and the transmission spectrum from a Yoldas type dry xerogel has been added, for means of comparison. An interesting result is that these FTIR spectra have patterns which parallel the XRD patterns, as a function of the sample type. For instance, if we consider the FTIR spectra of the Yoldas type xerogel labeled Y in Fig. 6, it shows the absorption bands labeled 1–4. We found that band 2 is present in all sol-gel materials made from nitrates, and therefore is typical of a Yoldas type gel made with HNO₃ in excess water. The three other bands progressively disappear as the samples transform to pseudo-boehmite (samples a1, a2 and c1), weak pseudo-boehmite (samples b1, c2 and c3), and amorphous (samples a3, b2 and b3). Simultaneously, bands 5–8 progressively appear. Possible attribution of these bands to etac side groups (Table III) indicates that the introduction of etac correlates with

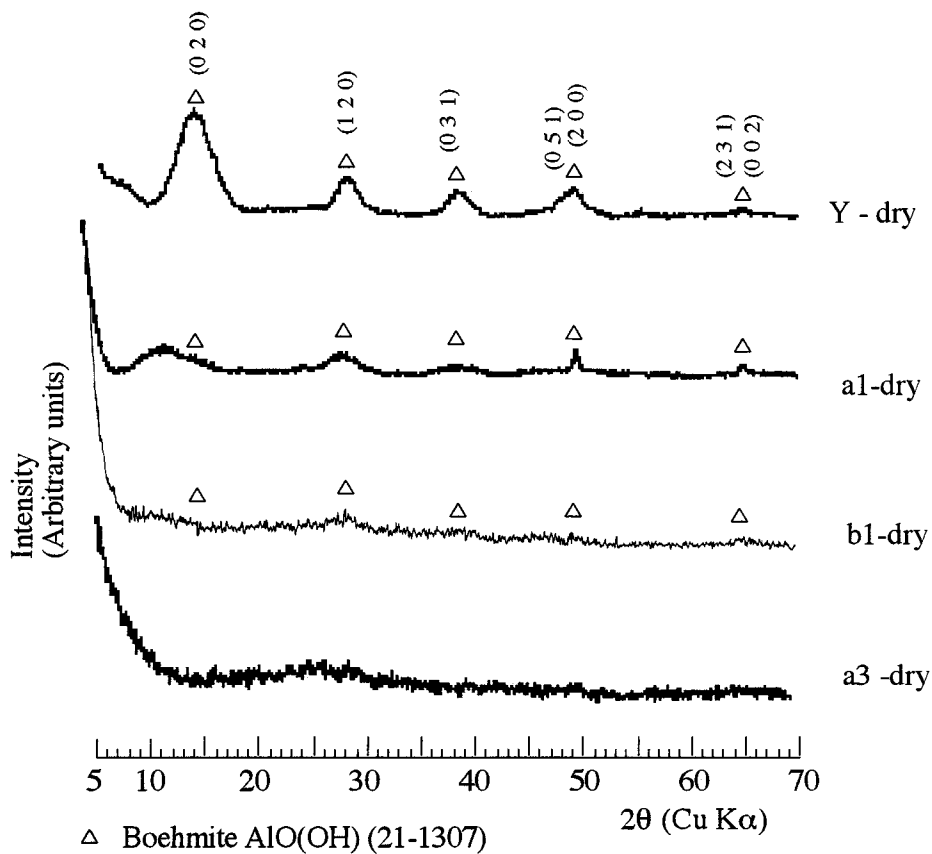


Figure 2 Typical powder X-ray diffraction patterns ($\text{CuK}\alpha$ radiation) of aerogels just after drying: Typical Yoldas type pseudo-boehmite xerogel (Y sample); Pseudo-boehmite type for aerogel sample a1 (similar patterns for a2 and c1); weak pseudo-boehmite type for aerogel sample b1 (similar pattern for c2 and c3); amorphous type for aerogel sample a3 (similar patterns for b2 and b3, AAa60/260 and AAa50/35).

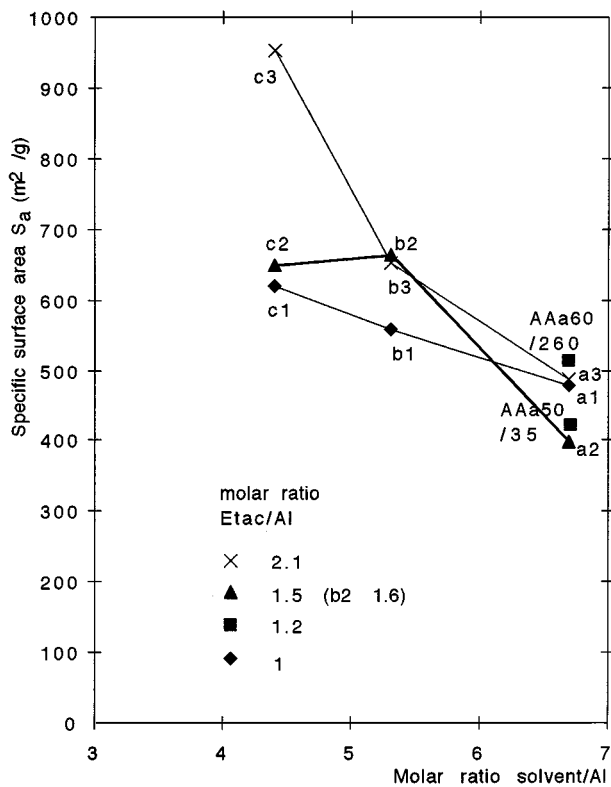


Figure 3 Evolution of the BET specific surface area of aerogels after drying and outgasing at $300\text{ }^\circ\text{C}$, as a function of the molar ratios $[\text{solvent}]/[\text{Al}]$ and $[\text{Etac}]/[\text{Al}]$.

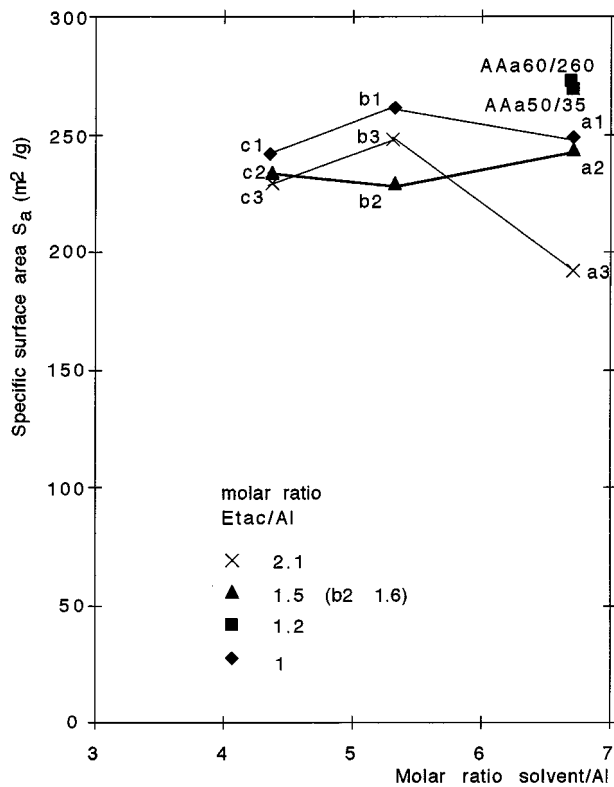


Figure 4 Evolution of the BET specific surface area of aerogels after heat treatment at $900\text{ }^\circ\text{C}$ in air, as a function of the molar ratios $[\text{solvent}]/[\text{Al}]$ and $[\text{Etac}]/[\text{Al}]$.

TABLE III Possible attribution of characteristic FTIR absorption bands of alumina gels made in this study

Band number	Wavenumber (cm ⁻¹)	Possible attribution and Wavenumber (cm ⁻¹)	Reference
1	1075	ν C-O from Al-butoxy groups, 1060	[5]
2	1384	nitrate anions	[6]
3	1639	ν C-O from Al-butoxy 1610, 1630	[5]
4	3086	ν C-H	[7]
5	1168	δ C-H from Al-etac groups	[5]
6	1459	δ CH ₃ from Al-etac groups	[5]
7	1567	ν C-C from Al-etac groups	[5]
8	2957	ν C-H	[7]

the progressive disappearance of the boehmite crystallographic structure.

The NMR spectra of samples Y, a1, b1 and a3 are reported in Fig. 7. Again, they show a transformation of spectra which is consistent with the XRD and FTIR data. The main peaks concerns Al^{VI}, in octahedral coordination sites. However, one small peak is present in the very weak boehmite type sample (b1) and the amorphous one (a3), respectively at ≈ 68 to 70 ppm which corresponds to Al^{IV} in tetrahedral coordination, [5, 6, 7].

4. Discussion

The present study first showed that complexing agents such as etac make it possible to directly obtain alumina aerogel monoliths by spontaneous gelation in an organic solvent, without requiring solvent evaporation as in the Yoldas technique [1]. Dry aerogels are very weak and must be handled with great care, but they be-

come translucent and much stronger transition alumina aerogel monoliths after thermal treatment at 900 °C.

The complexing agent used in this study, etac, obviously has a significant influence both on the gel network structure and on the pore texture of the dry aerogels, as these two characteristics change with the solvent/Al and etac/Al ratio. These results are consistent with previous studies by Simon *et al.* [8] and Yoldas [1] on alumina xerogels and by Pajonk [9] on aerogels who showed that the low temperature sol-gel synthesis and the drying conditions can have an important impact on the gel's pore texture and crystallographic structure. This is due to the fact, as showed by Keysar *et al.* [10], that aerogels made by supercritical drying in CO₂ (low temperature), aerogels made by supercritical drying at high temperature, and xerogels made by the Yoldas technique have a complex hierarchical aggregation architecture of primary particles in clusters which depends on the chemical conditions and particularly on the addition of an acid or a base. The solvent also is important and Grader *et al.* [11] made alumina aerogels with a fiber-like network texture by exchanging water for acetone in Yoldas type gels which they dried by the supercritical method in CO₂. As shown by Mizushima and Hori a fibrous texture also develops during supercritical drying at high temperature in alcohol [6, 7]. However, in the present study, while significant distinction could be made on the structure and pore texture of dry aerogels, these differences wiped out after thermal treatment at 900 °C.

Foreign elements, particularly organic complexing agents, are also known to have an important effect on the specific surface area [12], that is to say on the hierarchical organization of the gel network. In particular, etac is a chelating agent which is known to slow down the hydrolysis of Al-sb and modify the connectivity of the -Al-O-Al- network so as to significantly increase the residual specific surface area after heat treatment at temperatures as high as 1200 °C [13]. Therefore, in the

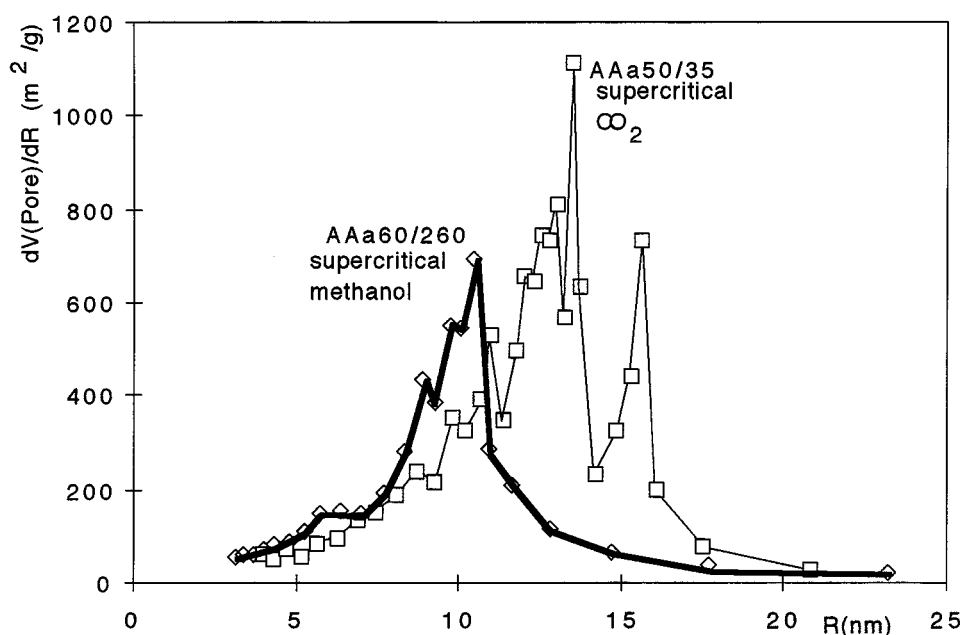


Figure 5 Compared pore size distribution of samples AAa60/260 and AAa50/35, derived from data on nitrogen adsorption according to the BET method in reference [2].

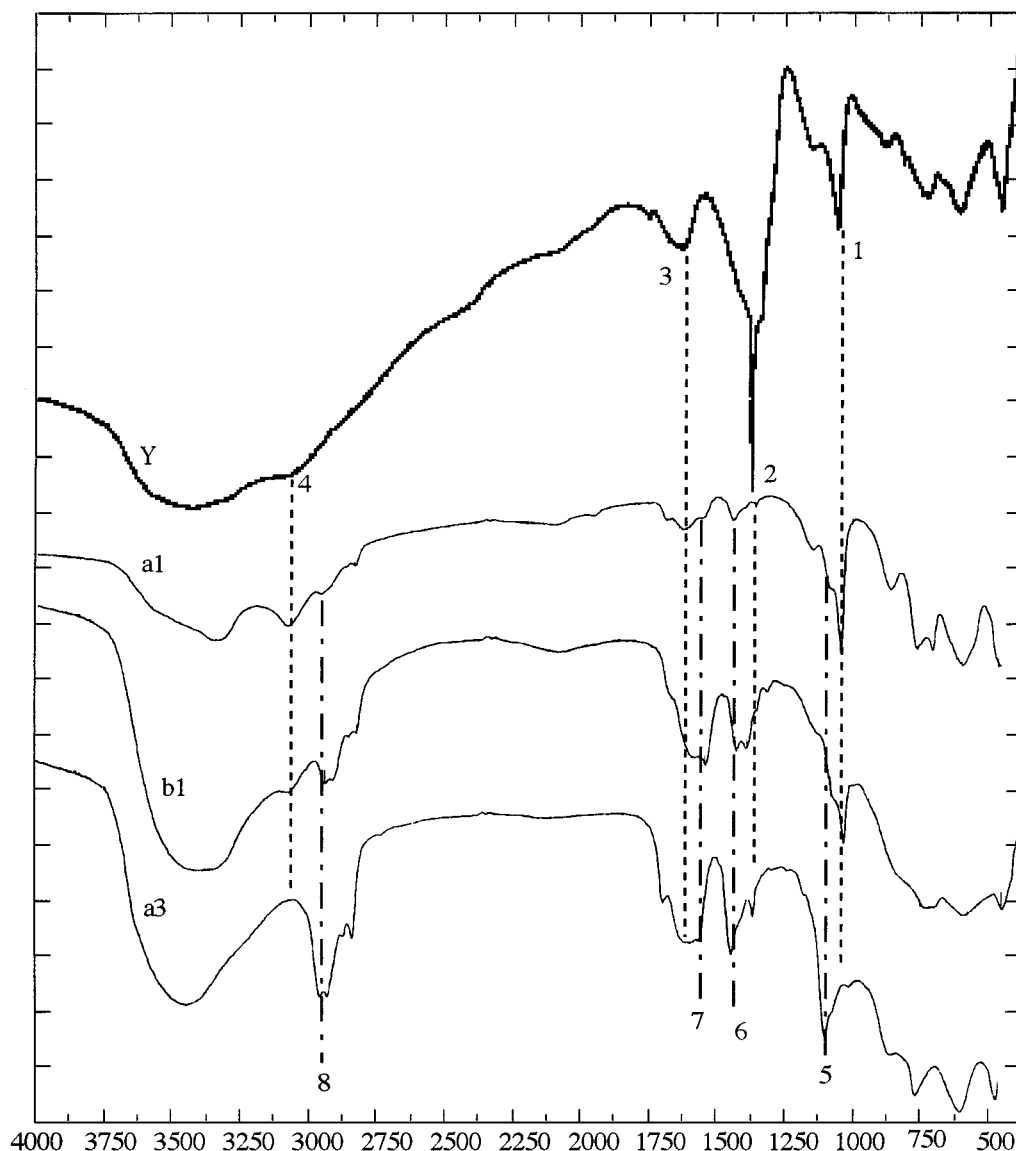


Figure 6 Infra-red transmission spectra of dry gels before heat treatment: in the wave vector range from 400 to 4000 cm^{-1} : (a) Yoldas type xerogel; (b) aerogel a1 (similar to a2 and c1); (c) aerogel b1 (similar to c3 and c2); and (d) aerogel a3 (similar to b2 and b3).

present study, it is not surprising that transparent materials could be made after heat treating some samples at 900 °C. A slower Al-sb hydrolysis rate was a key factor to succeed in making such transparent gels.

Three possibilities can be considered concerning etac, to explain the brown coloration of the aerogels after supercritical drying, and the strengthening of the A–O–Al network after thermal treatment at 900 °C.

First possibility, this additive could be completely eliminated from the Al ligand shell during supercritical drying and evacuated with the supercritical solvent, methanol. Second possibility, etac groups could remain linked to Al atoms in the aerogels, but as side groups only. That is to say they did not participate as Al-(etac)-Al bridges in active branches of the gel network. Third possibility, the etac groups could participate as active links in the aerogel network itself, to obtain a hybrid organic-inorganic gel.

The first possibility must be rejected on account of the FTIR data and on the fact that it is necessary to add some etac in order to obtain gel monoliths without solvent evaporation. In the second and third cases, etac

was likely to produce a carbonaceous residue which remained linked to the gel network, during supercritical drying at 260 °C and this was in agreement with the actual experimental observations. In the third case however, it would be unlikely to maintain a monolithic structure during heat treatment in air at 900 °C, or this monolithic structure would have weakened. Actually, the opposite evolution occurred as the gel monoliths became stronger. That is to say, not only the existing Al–O–Al bridges before thermal treatment did not disappear, but new ones were built. This is consistent with the fact that the formation of Al-(etac)-Al bridges would be an unlikely mode of coordination for a β -diketone.

This suggest that the second possibility is the right one, that is to say etac groups were only linked as side groups to the Al hydroxide gel network and they left $=\text{Al}-\text{O}-\text{C}\equiv$ side groups, responsible for a brown coloration after supercritical drying at high temperature (≈ 260 °C) in alcohol. This is also consistent with the fact that etac is not known to chelate Si precursors and no brown coloration remains in the base catalyzed silica aerogels after supercritical drying in alcohol [14].

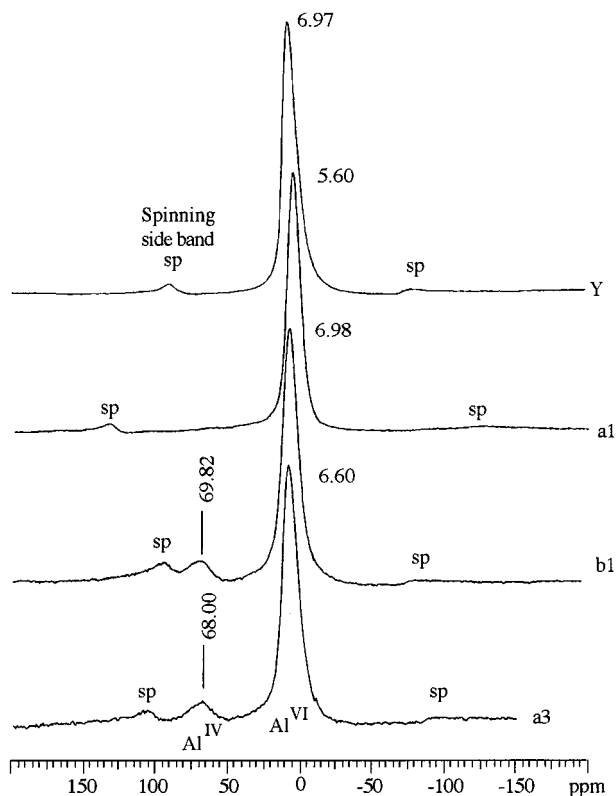


Figure 7 ^{27}Al NMR spectra of gels Y, a1, b1 and a3.

A comparison of the BET pore size distribution of samples dried by the supercritical technique in Fig. 5 shows that the dominating pore size decreased, from ≈ 14 nm. for supercritical drying in CO_2 at $\approx 35^\circ\text{C}$, to ≈ 10 nm for supercritical drying in methanol at $\approx 260^\circ\text{C}$. That is to say, a significant sintering occurred in supercritical fluid medium at 260°C , which explains that the gels could be handled as monoliths after supercritical drying at this high temperature, while only fluffy aggregates were obtained in CO_2 . It is also possible that this partial sintering was made possible by the removal of some organic links.

As reported in Fig. 2, the crystallographic structure just after drying was significantly different for all samples. In particular, maybe the most significant result of the present study is that the evolution in the XRD pattern correlated very well with both the evolution in the FTIR transmission and NMR patterns. These three sets of data indicated that when more etac groups entered into the ligand shell which surrounds each Al atom, new Al-etac absorption bands developed and simultaneously the boehmite crystallographic structure was more and more disrupted. The disruption first consisted in interlamellar boehmite swelling, then in the appearance of some Al^{IV} in tetrahedral coordination (Fig. 7), which resulted in a complete amorphous structure when more etac groups were linked to Al atoms.

Now, the relationship between these analytical data sets (XRD, FTIR and NMR) on one hand, and the chemical synthesis parameters ([etac]/[Al] and [solvent]/[Al] ratio) on the other hand, is not so clear. Roughly, it can be said that increasingly amorphous gels were obtained as the [etac]/[Al] ratio increased. But this only was a tendency in the present study, certainly because other

parameters, such as the temperature and the solvent/Al ratio have an importance.

Considering the temperature, it is well known that when the hydrolysis temperature is higher than 80°C , the formation of boehmite clearly occurs [1]. In the present study all reactants were first mixed at room temperature, then they were heated in a thermal bath at $\approx 60^\circ\text{C}$, which was necessary to obtain wet gels monoliths. But we also observed that boehmite patterns tend to develop slowly even in Yoldas types process carried out at this temperature. That is to say, nucleation and growth of boehmite also occurs at this temperature, although more slowly than above 80°C . In the present study, it is probably during this step that the most important uncontrolled fluctuations certainly occurred, especially concerning the time maintained at 60°C , in order to consolidate the wet gels strength, before storing them at room temperature for further supercritical drying, and this may have affected the germination/growth sequence of boehmite.

Moreover, the wet gels temperature was raised to $\approx 260^\circ\text{C}$ when performing supercritical drying in methanol, so that a partial dissolution-recrystallization may have occurred. It could be considered that such a dissolution should be easier when the [etac]/[Al] molar ratio is low and also when the [solvent]/[Al] ratio is high, hence a competition between these two synthesis parameters which is roughly consistent with our results. In details, in samples made with the highest solvent ratio and the lowest etac ratio (i.e., a1 and a2), the X-ray patterns of the gels were closer to that of boehmite, but with a significant shift to smaller 2θ angles of the (020) boehmite interlayer peaks, after supercritical drying. This is an indication that the side carbon groups were mostly intercalated in between the boehmite layers and that the formation of boehmite layers themselves was not disrupted. However, with an increasing [etac]/[Al-sb] and a decreasing [acetone]/[Al-sb] ratio, there was not enough solvent and/or too many etac groups to build large boehmite layers without disruption so that a more amorphous phase formed, with some Al in tetrahedral coordination.

We can note that this competition is well reflected by the data on the specific surface area of the aerogels. The specific surface area of the aerogel increased, to reach a value >900 m^2/g with the highest etac proportion ([etac]/[Al] molar ratio ≈ 2.1) and the lowest solvent proportion ([acetone]/[Al] molar ratio ≈ 4.5)

It would be interesting to derive a general guideline to make better transparent alumina aerogel monoliths. The present results showed that the transparency had a tendency to increase, in particular for samples of the series a and b, as the [etac]/[Al] ratio increased for the dry brown aerogel, and as this ratio decreased for the aerogels heat treated at 900°C . Stated differently, the most translucent brown samples after supercritical drying, tended to be the least transparent ones after heat treatment at 900°C . Again, this was only a tendency, imperfectly respected in details, probably due to the importance of other parameters such as the time at 60°C during wet gel synthesis. However, these general observations on the transparency of samples are consistent

with the role of etac to leave carbon side groups on the –Al–O–Al– gel network, after supercritical drying. A higher [etac]/[Al] ratio can be expected to leave smaller pores in the gel network, hence a better translucency of the brown dry aerogels, while it would leave larger pores after heat treatment at 900 °C, where all carbon atoms have left, hence a less transparent characteristics.

As for obtaining bigger uncracked alumina aerogel monoliths, the present study lets to consider that this should be possible. However, this requires to study more deeply the supercritical drying procedure itself, during which a more important relative shrinkage than for silica aerogels occurred.

5. Conclusions

Spontaneous gelation of aluminum alkoxide was obtained by decreasing the hydrolysis rate of this alkoxide by chelation with etac. Wet gels could be dried by the supercritical method to brown cracked aerogel monoliths. The handling strength of these monoliths increased significantly after heat treatment at 900 °C where they lost their coloration and became translucent. Consistent evolution in the XRD, FTIR and NMR data indicated that carbon side groups coming from etac remained in the aerogel, first in interlamellar position, then inside disrupted boehmite layers when they were responsible for the occurrence of Al atoms in tetrahedral coordination, as more etac was added. Hence, the specific surface area of aerogels dried by the supercritical method in methanol had a tendency to increase as

the [etac]/[Al] molar proportion increased and as the [solvent]/[Al] molar proportion decreased.

References

1. B. E. YOLDAS, *J. Mater. Sci.* **10** (1975) 1856.
2. A. C. PIERRE, E. ELALOUÏ and G. M. PAJONK, *Langmuir* **14** (1998) 66.
3. G. A. NICOALON and S. J. TEICHNER, *Bull. Soc. Chim. Fr* (1968) 1906.
4. S. J. TEICHNER, G. A. NICOLAON, M. A. VICARINI and G. E. E. GARDES, *Adv. colloid Interface Sci.* **5** (1976) 245.
5. F. BABONNEAU, L. COURY and J. LIVAGE, *J. Non-Cryst. Solids* **121** (1990) 153.
6. Y. MIZUSHIMA and M. HORI, *J. Non Cryst. Solids* **167** (1994) 1.
7. Y. MIZUSHIMA and M. HORI, "Eurogel '91," edited by S. Vilminot, R. Nass and H. Schmidt (Elsevier, 1992).
8. C. SIMON, R. BREDESEN, H. GRONDAL, A. G. HUSTOFT and E. TANGSTAD, *J. Mater. Sci.* **36** (1995) 5554.
9. G. M. PAJONK, *App. Cat.* **72** (1991) 217; *Catal. Today* **35** (1997) 319.
10. S. KEYSAR, Y. DE HAZAN, Y. COHEN, T. ABOUD and G. S. GRADER, *J. Mat. Res.* **12** (1997) 430.
11. G. S. GRADER, Y. RIFKIN, Y. COHEN and S. KEYSER, *J. of Sol-Gel Sci. and Technology* **8** (1997) 825.
12. Y. MIZUSHIMA, M. HORI and M. SASAKI, *J. Mat. Res.* **8** (1993) 2109.
13. Y. MIZUSHIMA and M. HORI, *ibid.* **8** (1993) 2993.
14. G. M. PAJONK, *J. Non Cryst. Solids* **225** (1998) 307.
15. K. NAKAMOTO, "Infrared and Raman spectra of inorganic and coordination compounds," John Wiley and Sons, New York, 1978.
16. S. REZGUI, B. C. GATES, S. L. BURKETT and M. E. DAVIS, *Chem. Mater.* **6** (1994) 2390.

Received 25 November 1998

and accepted 15 March 1999